A Self-tuning Regulator for the Voice Coil Motor

J. F. Pan[1], B.B.Yang[1,2], and Norbert Cheung[2]
[1] College of Mechatronics and Control Engineering, Shenzhen University.
[2]Department of Electrical Engineering, Hong Kong Polytechnic University.
3688, Nanhai Road, 518060, P.R.C.
pan_jian_fei@163.com

***Abstract*—A self-tuning regulator based on system identification and adaptive control is developed for the voice coil motor (VCM) to achieve high-precision control performance. With the aid of finite element methods (FEM), the characteristics of the VCM are investigated. Both the position response from numerical simulation and experimental results validate the effectiveness of the proposed control method and comparisons with a classical proportional integral differential (PID) controller are carried out. Experimental results testify the performance of the proposed regulator is better than that of the PID controller with absolute the steady state error of 3 um for the long stroke operation of 20 mm.**

***Index Terms*—system identification, adaptive control, FEM.**

I. Introduction

In recent years, miniature voice coil motors (VCMs) for ultra-high position control have been studied [1]-[2]. Though VCMs offer the advantages of simple and rigid structure, fast response and are expected to have large propulsion force and excellent dynamic response with small volume [3], the nonlinear behavior inherent from the magnetic paths prevents their applications in conventional, medium-stroke, position systems in manufacture and assembly industry [4].

In industrial operations, the working condition is often filled with different kinds of noise such as un-modeled parameter variations, un-measured dynamics and external load disturbances, etc. The PID algorithm is no longer capable of adaptation to such environment since it is based on the static model of the system [5]. Therefore, a control algorithm for disturbance detection and real-time compensation based on the dynamic model of the system should be introduced.

In this paper, characteristic analysis of a VCM with maximum stroke of 28 mm is performed. The online parameter identification with self-tuning regulation to correct uncertainties and disturbances in real-time are carried out. Control performance from the PID and the proposed regulator is verified by experimental results.

II. Modeling and Analysis

The machine structure of the VCM can be found as shown in Fig.1. Its stationary part consists of a foundry iron base, soft iron tube and three arched permanent magnets bonded in the base. The moving part is a plastic linear slide wounded with windings. The moving part is limited to the axial motion only between the air gaps. Major specifications can be found in Table I.

The relationship between electromagnetic force F and excitation current i can be characterized as,

$$F(x,t) = n \cdot K_1 \cdot B(x) \cdot l \cdot i(t). \quad (1)$$

where x is displacement and $B(x)$ is magnetic flux density. K_1, l and n represent the electromagnetic force coefficient, the conductor length per turn and the number of coil turns, respectively. The motion system can be represented as a typical second order system as,

$$m\ddot{x} + K_v\dot{x} + F_L = F(x,t) = K_f(x)i(t). \quad (2)$$

where m represents mass of the mover, K_v and F_L are the damping coefficient and load, respectively. It can be formulated in discrete-time transfer function form as [6],

$$G(z) = \frac{b_0 z + b_1}{z^2 + a_1 z^1 + a_2}. \quad (3)$$

where a_1, a_2 and b_0, b_1 represent the parameters of the system.

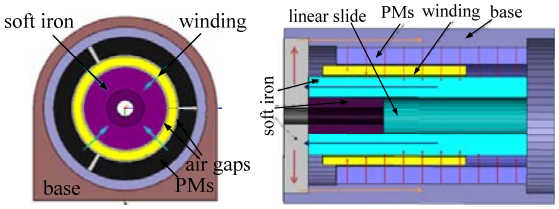

Fig. 1. Front view (a) and cut view (b) of the VCM

TABLE I
MAJOR SPECIFICATIONS

Parameter	Value
Mass of stator	1.0 kg
Mass of linear slide with coil	0.2 kg
Air gap length	0.2 mm
Number of turns	1000
Permanent magnet	NdFeB
Stator diameter	66.8 mm
Stator length	83.94 mm

III. Performance Prediction Based on FEM

The relationship from the force output to current levels and positions can be derived by FEM as shown in Fig.2 (a). Though K_f is not constant at the whole operation range, it can be regulated according to the position.

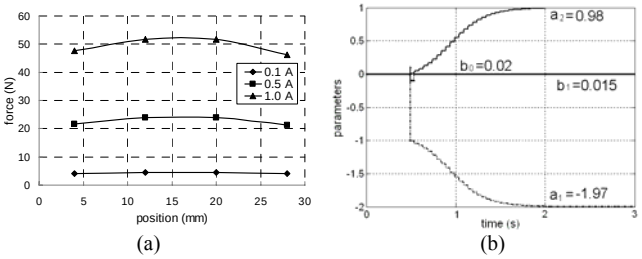

Fig. 2. Force calculation (a) and (b) parameter convergence profile

IV. Controller Design

A. Parameter Identification

As denoted in (3), a_1, a_2 and b_0, b_1 are parameters to be

estimated. Though disturbances may enter at any place into the control system with any form, for the *N*-th estimation, it can be considered as stochastic errors in least-square form as [6],

$$S_N = \phi_N \theta + e_N . \tag{4}$$

where $\theta = [a_1, a_2, b_1, b_2]$, $\phi_N = [-S_{N-1}, -S_{N-2}]$ and e is residuals. θ can be estimated by RLS algorithm as [5],

$$\begin{aligned} \hat{\theta}_{N+1=} &= \hat{\theta}_N + G_N[S_{N+1} - (\phi_{N+1})^T \hat{\theta}_N] \\ G_N &= \frac{P_N}{\rho + (\phi_{N+1})^T P_N \phi_{N+1}} \\ P_{N+1} &= \frac{1}{\rho}[I - G_{N+1}(\phi_{N+1})^T]P_N \end{aligned} . \tag{5}$$

where P is the covariance matrix and G is gain matrix. ρ is the forgetting factor. For initial values, $P = \sigma I$ as $\sigma = 20$ and I is the 4×4 unit matrix. The program termination criterion for recursive calculation can be set if the maximum proportion of error from the last and present is comparatively small. The parameters convergence profiles can be found in Fig.2 (b) and it takes about 1.5 s for all parameters to settle, which verify the effectiveness of the proposed parameter identification method.

B. Self-tuning Regulator Design

The regulator is designed based on pole-placement can be characterized as [6],

$$R \cdot u(t) = T \cdot F(t) - M \cdot S(t) . \tag{6}$$

and R , T , M are polynomials to be determined. The closed loop control output and system output can be represented as,

$$\begin{cases} S_{x(y)} = \dfrac{B(z^{-1})T(z^{-1})}{A(z^{-1})R(z^{-1}) + B(z^{-1})M(z^{-1})} \cdot F_{x(y)} + \dfrac{B(z^{-1})M(z^{-1})}{A(z^{-1})R(z^{-1}) + B(z^{-1})M(z^{-1})} \cdot v \\ u = \dfrac{B(z^{-1})T(z^{-1})}{A(z^{-1})R(z^{-1}) + B(z^{-1})M(z^{-1})} \cdot F_{x(y)} - \dfrac{B(z^{-1})M(z^{-1})}{A(z^{-1})R(z^{-1}) + B(z^{-1})M(z^{-1})} \cdot v \end{cases} . \tag{7}$$

Causality conditions are satisfied as,

$$\begin{cases} \deg A_c \geq 2 \deg A - 1 \\ \deg A_m - \deg B_m \geq \deg A - \deg B \end{cases} . \tag{8}$$

The closed loop characterization equation is represented as,

$$AR + BS = A_c = A_0 A_m . \tag{9}$$

and $A_m = z^2 + a_{m1} z^1 + a_{m2}$. A_m contains the desired closed loop poles. a_{m1} and a_{m2} can be obtained by the typical response from a second-order system and are set as -1.92 and 0.99, respectively. The control block diagram based on PID and the self-tuning regulator can be found in Fig.3.

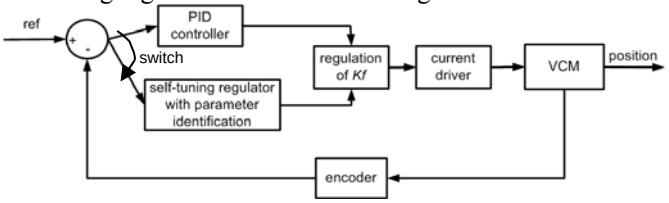

Fig. 3. Control block diagram

V. EXPERIMENTAL VERIFICATION

The experiment on position control of the VCM is carried out based on the dSPACE DS1104 controller card. As shown in Fig.4 the experimental setup, the whole experiment is conducted in real-time and the sampling frequency for position control loop is 1 KHz. The current driver is a commercial amplifier capable of inner current regulation based on PI algorithm with a sampling rate of 10 KHz. A linear magnetic encoder is mounted on the linear slide with a resolution of 1 μm.

The command reference square signal is 0.5 Hz with the amplitude of 20 mm. The dynamic response of adaptive control is shown in Fig.5. It is clear that the performance response under PID method is not uniform. However, for the self-tuning regulator, it is capable of uniform performance for both dynamic and static responses with an absolute steady state error of 3 μm. Experimental results prove that the control algorithm is capable of regulation to achieve a desired position response under the requirement of expected poles.

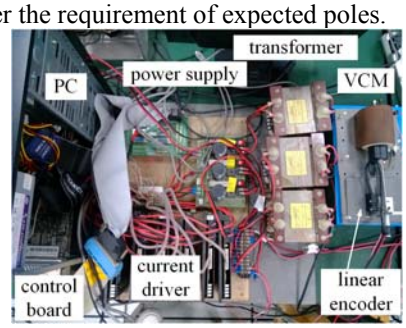

Fig. 4. Experimental setup

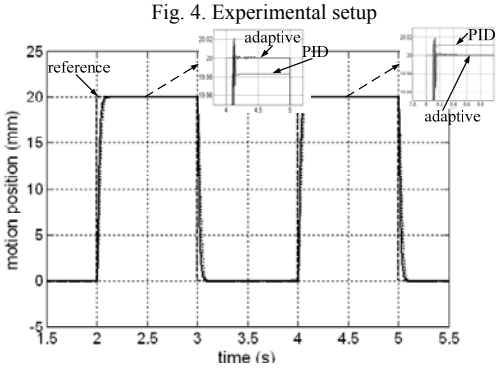

Fig. 5. Dynamic response under the self-tuning regulator and PID

VI. ACKNOWLEDGEMENT

The authors would like to thank the National Natural Science Foundation of China and Guangdong Natural Science Foundation for sponsoring of research projects under Grant 51007059, 51275312 and S2011010001208.

REFERENCES

[1] Jangwon Lee and Semyung Wang, "Topological shape optimization of permanent magnet in voice coil motor using level set method," *IEEE Trans. on Magn.*, vol. 48, no. 2, pp. 931-934, 2012.

[2] Hong Guo Dayu Wang and Jinquan Xu, "Research on a high-frequency response direct drive valve system based on voice coil motor," *IEEE Trans. on Power Electron.*, vol. 28, no. 25, pp. 2483-2492, 2013.

[3] Yu Liu, Ming Zhang, Yu Zhu, Jin Yang and Badong Chen, "Optimization of voice coil motor to enhance dynamic response based on an improved magnetic equivalent circuit model," *IEEE Trans. on Magn.*, vol. 47, no. 9, pp. 2247-2251, 2011.

[4] Chien-Sheng Liu, Psang-Dain Lin, Po-Heng Lin, Shun-Sheng Ke, Yu-Hsiu Chang and Ji-Bin Horng, "Design and characterization of miniature auto-focusing voice coil motor actuator for cell phone camera applications" *IEEE Trans. on Magn.*, vol. 45, no. 1, pp. 155-159, 2009.

[5] Lennart Ljung, *System Identification-Theory for the User*, 2nd ed., New York: Prentice-Hall, 1998, pp. 193-195.

[6] K. J. Åström and B. Wittenmark, *Adaptive Control*. 2nd ed., London: Addison-Wesley, 1995, pp.78-85.